Applied Mathematics & Information Sciences
An International Journal

http://dx.doi.org/10.12785/amis/080638

An Improved Unit-Linking PCNN for Segmentation of Infrared Insulator Image

Kebin Cui[1,*], *Baoshu Li*[2], *Jinsha Yuan*[3] *and Ping Wang*[1]

[1] Department of Computer , North China Electric Power University, 071000, Baoding, China
[2] Department of Electrical Engineering , North China Electric Power University, 071000, Baoding, China
[3] Department of electronics , North China Electric Power University, 071000, Baoding, China

Received: 8 Nov. 2013, Revised: 6 Feb. 2014, Accepted: 7 Feb. 2014
Published online: 1 Nov. 2014

Abstract: To segment the infrared insulator image efficiently, an improved Unit-linking PCNN algorithm, which makes improvements on both the linking coefficient β and the standard for choosing the best segmented image, is proposed in this paper. The relationship of the gray value of each neuron is used to determine the linking coefficient β and *MSE*, which consider the relationship between the gray value of the original image and the segmented image, is used to determine the best segmented image. The proposed algorithm is tested on both the standard test images and the aerial infrared images and the results show that the proposed algorithm gives better segmentation of the target image and better vision effect and less time are needed to get the best one.

Keywords: Unit-linking PCNN, segmentation, infrared image, MSE

1 Introduction

Inspecting line by helicopter is a new line maintenance method, which is efficient, fast, reliable, and cant be impacted by geographical factors. At present, China has carried out studies on Inspecting transmission line by helicopter. Infrared thermal imaging technology can convert the surface temperature of the invisible measured object to intuitive thermal images, which has been more widely used in the field of industrial measurement and control by virtue of its advantages such as non-contact, safe, reliable, fast and accurate. Inspecting by helicopters equipped with infrared cameras is used to transmission line inspection more and more. Analyzing the characteristics of the insulator is the basis to diagnosis, which requires segmenting the infrared image containing insulator. Image segmentation refers to the process to segment the image into regions each with features and extract the interest objects and it is a hot and difficult field of computer vision. The main methods for image segmentation includes clustering method [1,2,3], region growth approach [4], edge detection method [5] and multiseale gradient watersheds [6] etc. In recent years, pulse-coupled neural networks(PCNN) has sprung up as the third generation of neural network, which comes from the studies on the cat visual cortex [7,8,9].This signal processing mechanism has been widely used in image segmentation [10,11,12,13,14,15,16,17], feature extraction [18,19], object recognition [20,21,22] and image fusion [23,24,25,26] etc. However, there are many parameters which are difficult to assign in PCNN and the assignment of them has direct effect on the performance. To solve this problem, many simplified PCNN models are proposed by researchers, including the intersecting cortical model [27], the spiking cortical model (SCM) [28] and the unit-linking PCNN model [29], among which, Unit-Linking PCNN(UL-PCNN) has attracted many researchers by virtue of its simple assignment of parameters and better performance of segmentation and has been applied in some fields such as edge detection [30] and feature extraction [18] etc. But the solid value 0.2 of linking coefficient β cant reflect the linking relation between neurons accurately. In fact, the linking relation between neurons will vary as they are in different regions, of different gray value. In addition, UL-PCNN uses maximum Shannon entropy as a criterion to select the best segmented image, which will result in worse performance on the segmentation of infrared image with low contrast or low proportion of object. An improved UL-PCNN segmentation method called MUL-PCNN for

* Corresponding author e-mail: ncepuckb@163.com

infrared insulator image is presented in this paper, which can solve these two deficiencies of the UL-PCNN. MUL-PCNN gives better performance when the image is low contrast and has low proportion of object. Whats more, it is significant for the theoretical research and the standard for best segmented image selection in PCNN.

2 The PCNN model

The PCNN is a two-dimensional neural network. As shown in fig.1 [35], a neuron of PCNN consists of an input part, linking part and a pulse generator. [16,31,35] describe the definition of PCNN as Equ.(1)-(5):

$$F_{i,j}(n) = e^{-\alpha_F} F_{i,j}(n-1) + V_F \sum_{k,l} M_{i,j,k,l} Y_{k,l}(n-1) + S_{i,j} \quad (1)$$

$$L_{i,j}(n) = e^{-\alpha_L} L_{i,j}(n-1) + V_L \sum_{k,l} W_{i,j,k,l} Y_{k,l}(n-1) \quad (2)$$

$$U_{i,j}(n) = F_{i,j}(n)(1+\beta L_{i,j}(n)) \quad (3)$$

$$E_{i,j}(n) = e^{-\alpha_E} E_{i,j}(n-1) + V_E Y_{i,j}(n-1) \quad (4)$$

$$Y_{i,j}(n) = \begin{cases} 1, U_{i,j}(n) > E_{i,j}(n) \\ 0, U_{i,j}(n) \le E_{i,j}(n) \end{cases} \quad (5)$$

In these equations, Equ.(1) describes the model of feedback input subsystem, where $S_{i,j}$ is the input matrix of stimulus signals, usually corresponding with the gray value of image pixel in (i, j) position, $F_{i,j}(n)$ is the feedback input of the neuron in (i, j) in the nth time and $Y_{i,j}(n)$ is the binary output of the neuron. Equ.(2) describes the model of linking subsystem, where $L_{i,j}(n)$ is the linking input. The modulating subsystem is described in Equ.(3), where $U_{i,j}(n)$ is internal activation element and the dynamic threshold subsystem is described in Equ.(4), where $E_{i,j}(n)$ is the dynamic threshold. Equ.(5) describes the firing subsystem, where n is the number of the iterations, M and N are weight matrices(generally $M = N$) for linking input, α_L, α_E, and α_F are the attenuation coefficients of the dynamic threshold, linking input and feedback input, respectively, V_F, V_L and V_E are the range constant of $F_{i,j}(n)$, $L_{i,j}(n)$ and $E_{i,j}(n)$ respectively and β is the linking coefficient. When PCNN is used to image segmentation, the pixels of input image acts as neuron and the gray value of each pixel corresponds with $S_{i,j}$, the input of neuron. Assume the primary value of neuron is 1, in the first iteration, compare the internal activation $U_{i,j}(n)$ and the threshold $E_{i,j}$, if $U_{i,j}(n) > E_{i,j}$, the pulse generator will be activated and the neuron will be fired, an impulse or a sequence of impulses will be generated, which is called a "firing" and the output of the neuron is 1. After that, the threshold $E_{i,j}$ will be increased quickly by the feedback, when $U_{i,j}(n) \le E_{i,j}$ the impulse generator will be closed and stop generating impulse, the output of neuron will be 0, and then, the threshold $E_{i,j}$ will decreased exponentially with attenuation factor α_E, when $U_{i,j}(n) > E_{i,j}$, the neuron will be fired again, the output will be 1. This procedure will constantly continue. When a neuron is fired and generates an impulse, the pulse signal is transmitted to the adjacent neurons, the one having an approximate gray value will be fired rapidly and generate an impulse. Similarly, when a neuron flames out with the increase of the threshold, the adjacent one with an approximate gray value will flame out quickly. Thus, activation of a neuron may cause adjacent neurons with similar gray value activated naturally to form a cluster of similar neurons, which is corresponding to the area with similar characteristic in the image. It is based on this that the image segmentation can be performed.

3 The UL-PCNN model

The UL-PCNN model is a simplified model of PCNN proposed by Xiaodong, Gu. Improvement is made on the linking channel L and threshold E of PCNN. In PCNN, the composition of $L_{i,j}$ is so complicated that its change is related to the channel parameters of L and $Y_{i,j}$ consisted of the firing status of neurons, which makes the transmission very complex, meanwhile, the dynamic threshold is corresponding with α_E and V_E. To solve this problem, Unit-linking is introduced in [29], which means to each neuron, the signal of channel L $L_{i,j}$ will be 1 as long as there is a fired neuron in its neighborhood(not including the core neuron itself), otherwise $L_{i,j}$ will be 0. In UL-PCNN, a fired neuron will fire any unfired neurons with similar gray value in its neighborhood, thus, the transmission of signal is clear and easy to manage. $L_{i,j}$ is described by Equ.(6):

$$L_{i,j}(n) = \begin{cases} 1, \sum_{k \in N(ij)} Y_k(n-1) > 0 \\ 0, \sum_{k \in N(ij)} Y_k(n-1) = 0 \end{cases} \quad (6)$$

where, $N(ij)$ represents the neighborhood of (i, j). To simplify the computation, matrix E is replaced by a constant matrix and the value will decay by a positive attenuation constant δ not by exponent. The simplified equation is Equ.(7).

$$E_{i,j}(n) = E_{i,j}(n-1) - \delta + V_E Y_{i,j}(n-1) \quad (7)$$

To get the best results, the image is segmented twenty times from high gray value to low gray value, a binary matrix is got in each iteration as the result of segmentation. The optimal segmented image is selected by the image's Shannon entropy as defined by Equ.(8). The one with the largest image's Shannon entropy is the optimal one and will be used as the final result of segmentation.

$$H = -P_0 \log_2 P_0 - P_1 \log_2 P_1 \quad (8)$$

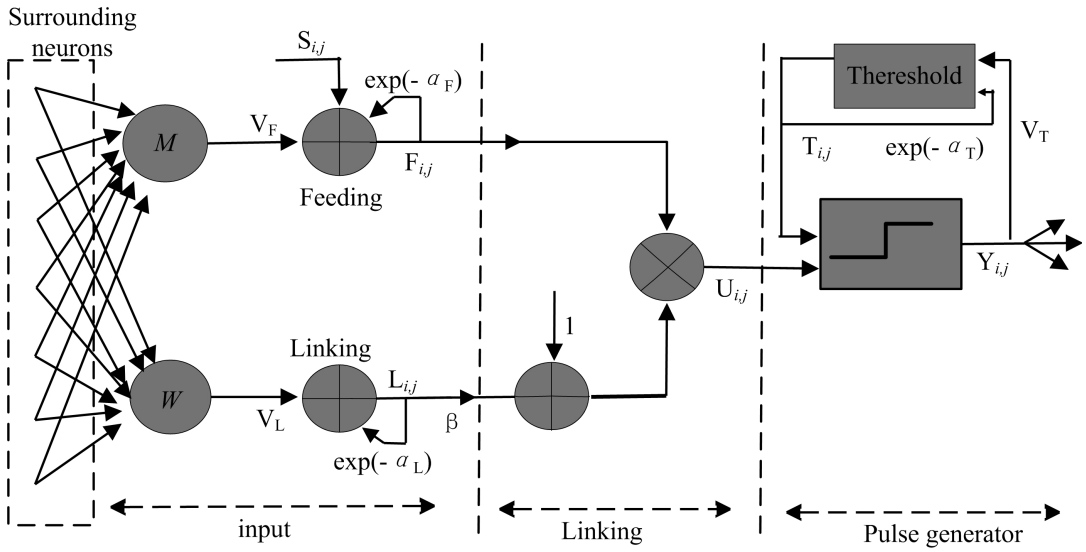

Fig. 1: PCNN'S neuron model

where P_0 and P_1 represent the probability of the segmented image whose intensity is 0 and 1, respectively.

The algorithm based on UL-PCNN is as follow:

Step 1: Normalize the Original image. Assume $L = U = Bin = 0$, $E = 1$. Meanwhile, each pixel does not fire, that is, $Y = 0$. Assume $N = 20$, $\beta = 0.2$, $\delta = 1/20 = 0.5$, $V_E = 100$(to prevent the fired neuron from firing again, normally bigger than 1), $K = [1\ 1\ 1; 1\ 0\ 1; 1\ 1\ 1]$.

Step 2: $L = conv2(Y, K, 'same')$, $L = step(L)$, $Inter = Y$, $U = F. * (1 + . * L)$, $Y = step(step(U - E) + Y)$, where, conv2 represents the convolution function and step represents the step function.

Step 3: If $Inter = Y$, go to step4, else, go back to step 2.

Step 4: If $Y(i, j) = 1$, then $Bin(i, j) = 1 (i = 1, \cdots, r; j = 1, \cdots, c)$. where , $Y(i, j)$ and $Bin(i, j)$ are elements of Y, Bin respectively. r is the height of the image. c is the width of the image.

Step 5: $E = E - \delta + V_E * Y$. On one hand, decrease threshold with the increase of N. On the other hand, prevent the fired neuron from firing again.

Step 6: Calculate the image Shannon entropy of Bin. Save the Bin which has the maximum image Shannon entropy till now as Res. When the algorithm is finished, Res is the final result.

Step 7: $N = N - 1$, if $N \neq 0$, go back to step 2, else end.

The characteristic of this method is that there are fewer parameters and they are relative solid, such as $\beta = 0.2$, $\delta = 1/20 = 0.5$, $V_E = 100$, so it can automatically and efficiently segment images without choosing different parameters for different kinds of images. However, the solid parameters bring forth some shortcomings:

1) β is linking coefficient which represents the coupling intensity of the neuron and the neurons in its neighborhood, which reflects the difference of them to fire the approximate neurons. As we all know each image has its own characteristic, a solid value 0.2 is not rational for representing this linking.

2) From the definition of the image Shannon entropy, as shown in Equ.(8), H can get its maximum when $P_0 = P_1$, which means that the segmented image with same quantities of 0s and 1s is the best one. It is very suitable for segmenting the image in which the object and background are of equal proportions not for all the images, especially for the image whose background and object is far from equal. In addition, the image's Shannon entropy is calculated on the segmented image, not considering the original one. In fact, the performance of segmentation should be evaluated by comparison of the original image and the segmented image, which can give better vision effect.

4 Improved UL- PCNN segmentation for infrared insulator image

To overcome the main shortcomings of UL-PCNN described in last section, improvements are proposed in this paper. For the solid value of β, the local mean variances between each neuron and its neighbors are used to describe the linking coefficient β, that is, the linking coefficient β_{ij} of the neuron(i,j) is defined as Equ.(9).

$$\beta_{ij} = \sigma = (\sum_{k=1}^{3}\sum_{l=1}^{3}(x_{kl} - \bar{x}_{ij})^2/n)^{1/2} \quad (9)$$

where, x_{kl} represents the gray value of the neuron in the neighborhood of neuron(i,j), $\bar{x}_{ij}$ represents the average value of all the neurons in $k \times l$ neighborhood of neuron(i,j) and n is the number of neurons in the $k \times l$ neighborhood. It can be concluded that, β_{ij} represents the dispersion between the values of the neurons in neuron(i,j)'s neighborhood and the mean value of them from Equ.(9). The smaller it is, the less straggling the neurons are, the closer their values to the average value $\bar{x}_{ij}$. On the contrary, the larger it is, the more straggling they are, the larger distance between they and the average value. However, in essence, β_{ij} is the linking between the neuron and neurons in its neighborhood. That is, the dispersion between the neuron and neurons its neighborhood, not between the mean value and the neurons, can reflect the linking more accurately. In this paper, a new definition of β_{ij} is proposed as Equ.(10).

$$\beta_{ij} = \sigma_{(i,j)} = (\sum_{k=1}^{3}\sum_{l=1}^{3}(x_{kl} - x_{ij})^2/n)^{1/2} \qquad (10)$$

where, x_{ij} is used to replace $\bar{x}_{ij}$ in Equ.(9), thus β_{ij} represents the dispersion between the neuron and neurons in its neighborhood. The smaller it is, the less straggling between the neuron and neurons in its neighborhood, the easier the neuron to be fired; the larger it is, the more straggling between the neuron and neurons in its neighborhood, the more difficult the neuron to be fired.

To evaluate the performance of segmentation, both the origin image and the segmented image are important. In this paper, we use mean square error(MSE) to determine the final result of segmentation. MSE is described in Equ(11):

$$MSE = \frac{1}{MN}\sum_{i=1}^{M}\sum_{j=1}^{N}||X_{ij} - Y_{ij}||^2 \qquad (11)$$

where, X_{ij} and Y_{ij} represent the gray value of pixel(i,j) in original image and segmented image, respectively. Because the segmented image is a binary image, the value of Y_{ij} is 0 or 1, the original image should be normalized before calculating MSE. The smaller MSE is, the more similar the original image and the segmented image are, whereas, the larger the more different. The segmented image which has the smallest MSE will be the final result of segmentation by MUL-PCNN.

5 Experiments and analysis

To testify the efficiency of the proposed algorithm, tests are done on both the standard test image pepper.jpg(512×512) and a infrared insulator image insulator.jpg(704×576) captured from aerial video.

5.1 Test on pepper.jpg

Assume the number of iteration is 20, both the algorithm based on UL-PCNN and MUL-PCNN will generate 20 segmented images. Fig.2 shows the first, third, fifth, seventh, ninth, eleventh and thirteenth segmented image of the two algorithm and the line charts of the image Shannon entropy and MSE of the 20 segmented images are shown in Fig.3 and Fig.4, respectively.

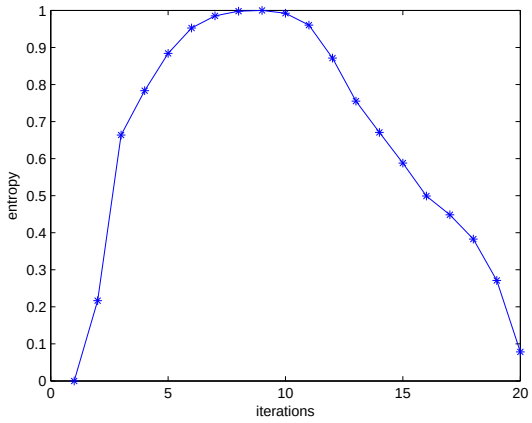

Fig. 3: the line chart of the image entropies of segmented images by UL-PCNN for pepper.jpg

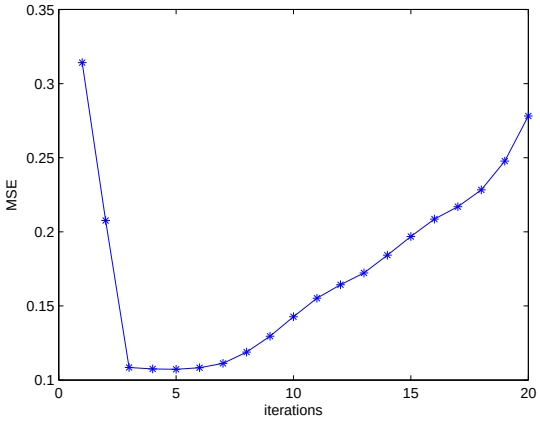

Fig. 4: the line chart of MSE of segmented images by MUL-PCNN for pepper.jpg

It can be concluded from Fig.3. that the ninth segmented image by UL-PCNN will be chosen the best segmented one, which locates in row 1 column 5. While, Fig.4. shows that the fifth segmented image by

Fig. 2: the segmented images of pepper by UL-PCNN(the first row) and MUL-PCNN(the second row)

MUL-PCNN will be chosen the best segmented one, which locates in row 2 column 3. The two selected segmented images are list below as Fig.5 and Fig.6.

Fig. 5: the optimal segmented image by UL-PCNN

Compare Fig.5 and Fig.6, the segmentation results are comparative. However, to get the optimal one, nine iterations are done by UL-PCNN, only 5 iterations by MUL-PCNN which can be conclude from Fig.3 and Fig.4. In addition, neurons can be fired faster by MUL-PCNN than by UL-PCNN. At the same iteration, more neurons are fired by MUL-PCNN than by UL-PCNN, which results in getting optimal segmented image quickly by MUL-PCNN.

5.2 Test on insulator.jpg

There are equal proportion of object and background in pepper.jpg, so the performance of UL-PCNN and MUL-PCNN has no obvious difference. However, There

Fig. 6: the optimal segmented image by MUL-PCNN

are many images whose object and background are far from equal, such as the infrared insulator image, in which the object insulator occupy small proportion and far from equal to the background, as shown in Fig.7.

To analyze the characteristic of insulator in Fig.7, segmentation is needed. But the shoot parameters kept in Fig.7 may disturb the segmentation, so it must be handled before segmentation. The erodent of set is used to remove these shoot parameters, Fig.8 shows the image after handling.

Just as test the pepper.jpg, both the algorithm based on UL-PCNN and MUL-PCNN generate 20 segmented images. Fig.9 shows the first, fourth, seventh, tenth, thirteenth, sixteenth and nineteenth segmented image of the two algorithms and the line charts of the image Shannon entropy and MSE of the 20 segmented images are shown in Fig.10 and Fig.11, respectively.

From Fig.10 and Fig.11, we can conclude that the sixteenth segmented image is the optimal one selected by UL-PCNN. And the fourth segmented image is selected

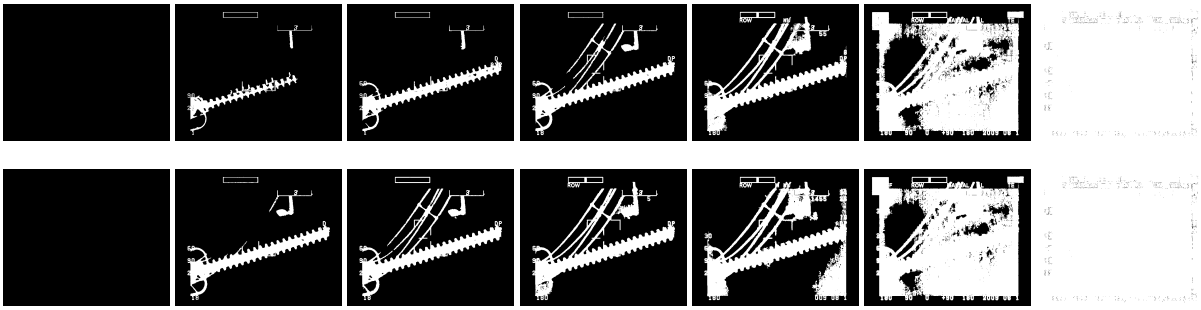

Fig. 9: the segmented images of pepper by UL-PCNN(the first row) and MUL-PCNN(the second row)

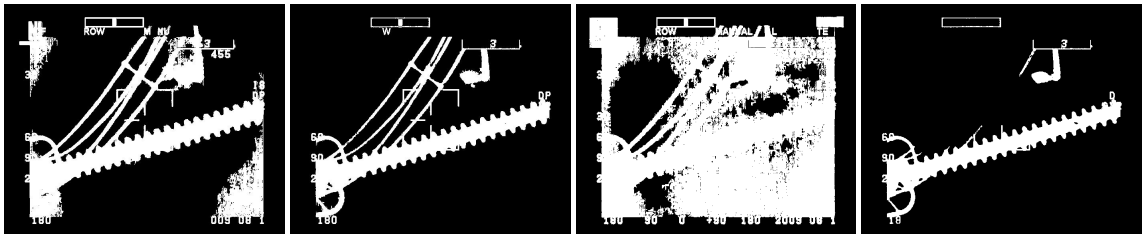

Fig. 12: the effects of four algorithms: the minimum cross entropy, OTSU, UL-PCNN and MUL-PCNN from left to right

Fig. 7: the infrared insulator image

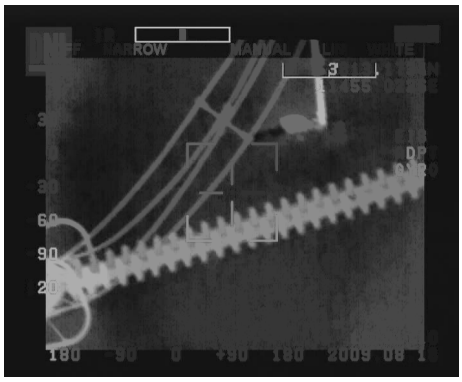

Fig. 8: the infrared insulator image without shoot parameters

as the optimal by MUL-PCNN. Obviously, MUL-PCNN has better performance than UL-PCNN, whats more, less iterations are needed to gain the optimal one.

From the results of these two tests on pepper.jpg and insulator.jpg, it can be concluded that MUL-PCNN can fire the neuron faster because β_{ij} used the mean variance between neuron and its neighbors and improvements have been made on both effect and numbers of iteration by using MSE as the criterion of selecting the optimal segmented image. Fig.10 shows that the change of the value of MSE is a concave function as a whole, so it can be used to determine whether to continue the iteration, that is, if it is larger than last time, the iteration can finish, which would greatly reduce the execution time.

To evaluate the proposed algorithm efficiently, comparisons are also be made with minimum cross entropy thresholding in [33] and OTSU in [34]. The results are shown in Fig.12.

Fig.12 shows that the optimal segmented image selected by the proposed algorithm shows the best vision effect and has the most clear object edges, while, the worst effect is got by UL-PCNN, the selected images by the minimum cross Shannon entropy and OTSU keep the edges of both the object and some other things in the

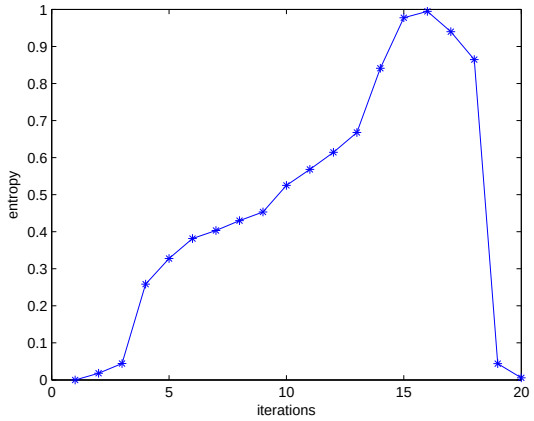

Fig. 10: the line chart of the image entropies of segmented images by UL-PCNN for insulator.jpg

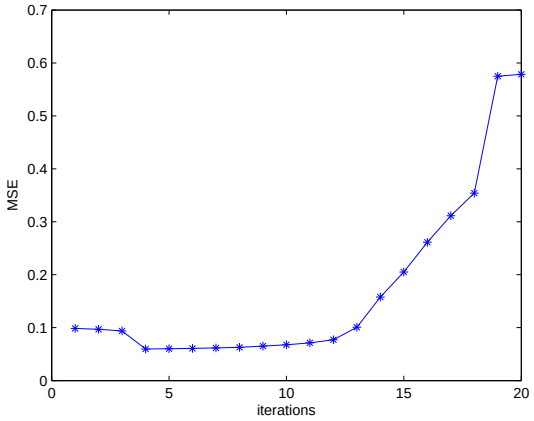

Fig. 11: the line chart of MSE of segmented images by MUL-PCNN for insulator.jpg

original image which we are not caring about and can confuse us when analyzing the object later.

6 Conclusion

A new algorithm MUL-PCNN based on UL-PCNN is proposed in this paper, which setting the value of β based on the relationship between the core neuron and its neighbors, which results in fast firing. MSE is used as the criterion to select the optimal segmented image in proposed algorithm, which makes the algorithm suitable for not only the images with equal proportion of object and background, but also the images with unequal proportion. The results of comparisons with UL-PCNNthe minimum cross Shannon entropy and OTSU show the proposed algorithm gives better vision effect and can keep the edges of object well.

Acknowledgements

This study was supported by the Fundamental Research Funds for the Central Universities (N0. 2014MS134).

References

[1] Ran Wehrens, Lutgarde M C Buydens, Chris Fraley, Adrian E Raftery, Model-Based Clustering for Image Segmentation and Large Datasets via Sampling, Journal of Classification, **21**, 231-253 (2004)

[2] S. Colantonio, O. Salvetti, and I.B. Gurevich, A two-step approach for automatic microscopic image segmentation using fuzzy clustering and neural discrimination, Pattern Recognition and Image Analysis, **17**, 428-437 (2007).

[3] Z.X. Ji, Q. Chen, Q.S. Sun, and D.S. Xia, Image Segmentation with Anisotropic Weighted Fuzzy C-Means Clustering, Journal of Computer-Aided Design & Computer Graphics, **21**, 1451-1459 (2009).

[4] H.Y. Quan and T.W. Zhang, Region Growth Approach for Mesh Model Segmentation, Journal of Computer-Aided Design & Computer Graphics, **18**, 1011-1016 (2006).

[5] M Chapron, A new chromatic edge detector used for color image segmentation, Proc. of the 11th International Conference On Pattern Recognition, Hague, 311-314 (1992).

[6] I Vanhamel, I Pratikakis, and H Sahli, Multiseale gradient watersheds of color images, IEEE Transactions on Image Processing, **12**, 617-626 (2003).

[7] ckhorn R, Reit boeck H J, and A rndtetal M, Feature linking via synchronization among distributed assemblies : simulation of results from cat cortex, Neural Computation, **2**, 293-307 (1990).

[8] R. Eckhorn, H. J. Reitboeck, M. Arndt, and P. W. Dicke, A neural network for feature linking via synchronous activity: Results from cat visual cortex and from simulations, Models of Brain Function. Cambridge, 255-272 (1989).

[9] J. Reitboeck, R. Eckhorn, M. Arndt, and P.W. Dicke, A model of feature linking via correlated neural activity, Synergistics of Cognition, New York, 112-125 (1989).

[10] G. Kuntimad and H.S. Ranganath, Perfect image segmentation using pulse coupled neural networks, IEEE Trans. Neural Netw., **10**, 591-598 (1999).

[11] R.D. Stewart, I. Fermin, and M. Opper, Region growing with pulsecoupled neural networks: An alternative to seeded region growing, IEEE Trans. Neural Netw., **13**, 1557-1662 (2002).

[12] J.A. Karvonen, Baltic sea ice SAR segmentation and classification using modified pulse-coupled neural networks, IEEE Trans. Geosci. Remote Sens., **42**, 1566-1574 (2004).

[13] Y. Bi, T. Qiu, X. Li, and Y. Guo, Automatic image segmentation based on a simplified pulse coupled neural network, Advances in Neural Networks, Berlin, 199-211 (2004).

[14] Y.D. Ma and C.L. Qi, Study of automated PCNN system based on genetic algorithm, J. Syst. Simul., **18**, 722-725 (2006).

[15] Y. Lu, J. Miao, L. Duan, Y. Qiao, and R. Jia, A new approach to image segmentation based on simplified region growing PCNN, Appl. Math. Comput., **205**, 807-814 (2008).
[16] H. Berg, R. Olsson, T. Lindblad, and J. Chilo, Automatic design of pulse coupled neurons for image segmentation, Neurocomputing, **71**, 1980-1993 (2008).
[17] M. Yonekawa and H. Kurokawa, An automatic parameter adjustment method of pulse coupled neural network for image segmentation, Proc. Artif. Neural Netw., Limassol, 834-843 (2009).
[18] J. Zhang, K. Zhan, and Y. Ma, Rotation and scale invariant antinoise PCNN features for content-based image retrieval, Neural Netw.World, **17**, 121-132 (2007).
[19] X. Gu, Feature extraction using unit-linking pulse coupled neural network and its applications, Neural Process. Lett., **27**, 25-41 (2008).
[20] J.M. Kinser and J.L. Johnson, Object isolation, Opt. Memor. Neural Netw., **5**, 137-145 (1996).
[21] H.S. Ranganath and G. Kuntimad, Object detection using pulse coupled neural networks, IEEE Trans. Neural Netw., **10**, 615-620 (1999).
[22] B. Yu and L. Zhang, Pulse-coupled neural networks for contour and motion matchings, IEEE Trans. Neural Netw., **15**, 1186-1201 (2004).
[23] R.P. Broussard, S.K. Rogers, M.E. Oxley,and G.L. Tarr, Physiologically motivated image fusion for object detection using a pulse coupled neural network, IEEE Transactions on Neural Networks, **10**, 554-563 (1999).
[24] E.P. Blasch, Biological information fusion using a PCNN and belief filtering, Proc. of International Joint Conference on Neural Networks, Washington, 2792-2795 (1999).
[25] B. Xu and Z. Chen, A multisensor image fusion algorithm based on PCNN, Proc.of the 5th World Congress on Intelligent Control and Automation, 3679-3682 (2004).
[26] W. Li and X. Zhu, A new image fusion algorithm based on wavelet packet analysis and PCNN, Proc. of the 4th International Conference on Machine Learning and Cybernetics, Guangzhou, 5297-5301 (2005).
[27] T. Lindblad and J. M. Kinser, Image Processing Using Pulse-Coupled Neural Networks, New York, (2005).
[28] K. Zhan, H. Zhang, and Y. Ma, New spiking cortical model for invariant texture retrieval and image processing, IEEE Trans. Neural Netw., **20**, 1980-1986 (2009).
[29] X.D. Gu, S.D. Guo and D.H. Yu, a new approach for automated image segmentation based on unit-linking pcnn, Proc. of the First International Conference, Beijing, 175-178 (2002).
[30] X. Gu, L. Zhang, and D. Yu, General design approach to unit-linking PCNN for image processing, Proc. Int. Joint Conf. Neural Netw., Montrealvol, 1836-1841 (2005).
[31] Shuo Wei, Qu Hong and M.S. Hou, Automatic image segmentation based on PCNN with adaptive threshold time constant, Neurocomputing, 1485-1491 (2011).
[32] N. Yang, H.J. Chen and Y.F. Li, Coupled Parameter Optimization of PCNN Model and Vehicle Image Segmentation, Journal of Transportation Systems Engineering and Information Technology, **12**, 48-54 (2012).
[33] C.H. Li and C.K. Lee, Minimum cross entropy thresholding, Pattern Recognition, **26**, 617-625 (1993).
[34] Nobuyuki Otsu, A Threshold Selection Method from Gray-Level Histograms, IEEE Transactions on Systems, Man and Cybernetics, **9**, 62-66 (1979).
[35] Z.B Wang, Y.D. Ma,F.Y. Cheng, L.Z. Yang, Review of pulse-coupled neural networks, Image and Vision Computing, **28**, 5-13 (2010).

Kebin Cui is currently pursuing the Ph.D. degree from the Department of Electrical Engineering, North China Electric Power University, Baoding, China. He is currently a Lecturer with the Department of Computer, North China Electric Power University, His research interests are the application of image processing in electric power system, including image denoising, image segmentation, feature extraction, image fusion and so on.

Baoshu Li is currently a Professor with the Department of Electrical Engineering, North China Electric Power University, Baoding China. His research interests are in the areas of image processing technology in power system applications, technology and power of modern electromagnetic measuring and Electrical equipment condition monitoring.

Jinsha Yuan is currently a Professor with the Department of Electronic, North China Electric Power University, Baoding China. His research interests are in the areas of image processing technology in power system applications, Computer information processing and Electromagnetic Calculation

Ping Wang is currently a Lecturer with the Department of Computer, North China Electric Power University, Baoding China. Her research interests are in the areas of image denoising, image segmentation and Artificial intelligence.